

A satellite-style map of North America, showing the United States and parts of Canada. The map is overlaid with numerous small red dots, primarily concentrated in the central and eastern United States, representing simulation locations. The text is overlaid on the map in yellow and white.

Fire dynamics during the 20th century simulated by the Community Land Model

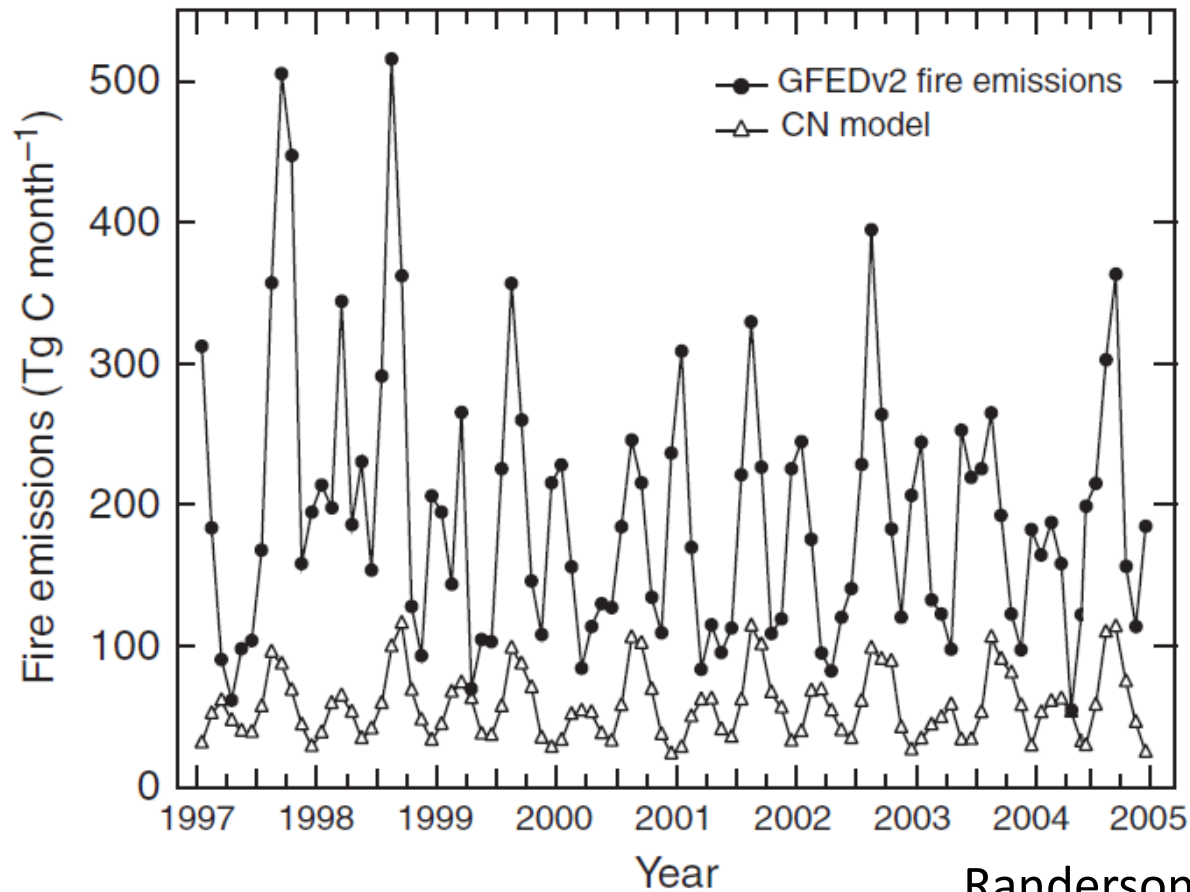
S. Kloster, N. M. Mahowald, J. T. Randerson, P. E. Thornton,
F. M. Hoffman, S. Levis, P. J. Lawrence, J. J. Feddema,
K. W. Oleson, and D. M. Lawrence

NCAR

Joint Land and BGC Working Group Meetings

10 February 2010

Fires emissions in C-LAMP version of CLM-CN were too low



Randerson et al. (2009)

Fire emissions difficult to simulate:

Requires correct distribution of NPP, aboveground biomass, burned area, fuel moisture levels, combustion completeness, ignition sources

Adjustments to fires in CLM-CN

- Move from a Thonicke et al. (2001) LPJ algorithm to one proposed by Arora and Boer (2005)
 - First step is to estimate burned area as a function of climate and fuel loads
 - Thonicke et al. (2001) estimated burned area empirically as a function of fire season length
 - Arora and Boer algorithm estimates fire spread rates using wind speed and fuel moisture (top 5 cm soil moisture) each day
 - Potential burned area reduced by probabilities of fuel load and ignition
 - Emissions then estimated by: $E = A \times C \times cc \times mort$
 - Combustion completeness and mortality differ for different pfts and pools
 - Ignition probability modified to include human ignition and suppression as a function of time-varying population density in each grid cell
- Deforestation fires now represented
 - Conversion flux from land use now enters a pool that is either combusted or decomposed depending on fire weather; may accumulate over time
 - Captures seasonal and interannual variations in deforestation emissions
- Performed transient simulations from 1798 to 2004
- Paper in Biogeosciences Discussion at <http://www.biogeosciences-discuss.net/7/565/2010/bgd-7-565-2010.pdf>

Burned area in some regions observed to have highest levels at intermediate levels of population density

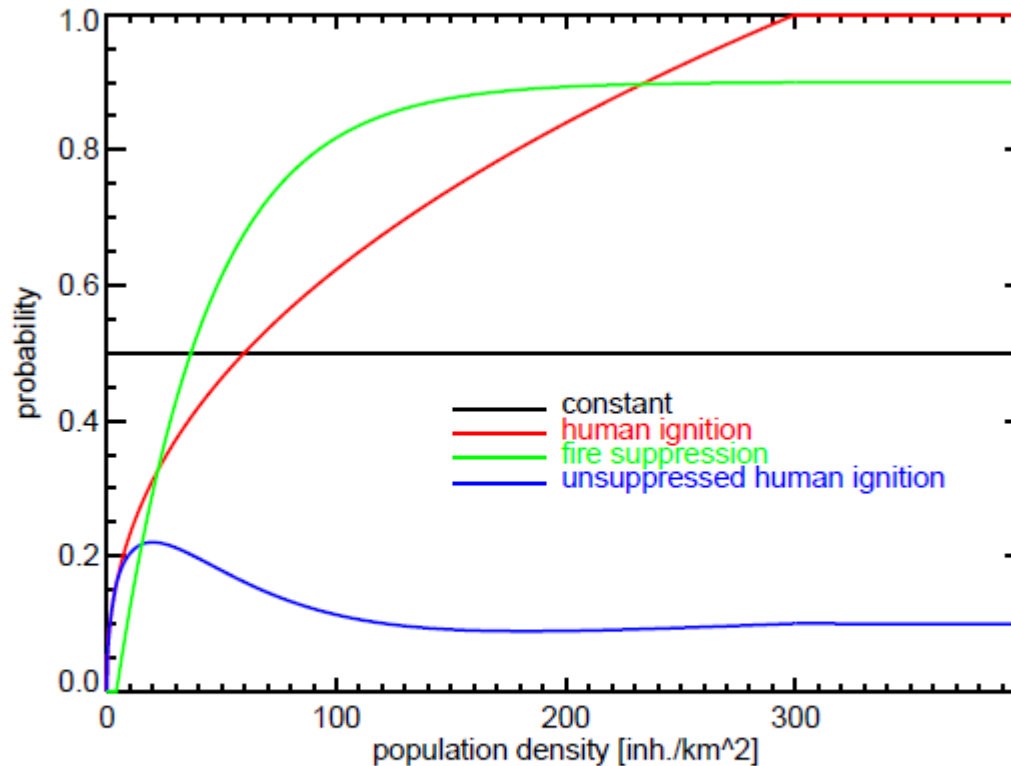


Fig. A1. Human ignition probability and fire suppression [0–1] as function of population density [inhabitants/km²]. Black: constant ignition probability; red: Human ignition probability; green: fire suppression; blue: unsuppressed human ignition (human ignition*(1–fire suppression)).

Table 1. Control and transient model simulations analyzed in the present study. Simulations use different fire algorithms, different treatment of human ignition potential, and different assumptions about land-cover change and wood harvest as well as climate forcing.

Name	Fire algorithm ¹	human ignition ²	pop. density ³	Land-cover change ⁴	CO ₂ concentration/ Nitrogen deposition ⁵	Climate forcing ⁶
Control simulations						
C-T	Thonicke	–	–	–	pre-industrial	1948–1972
C-AB	Arora and Boer	constant=0.5	–	–	pre-industrial	1948–1972
C-AB-HI	Arora and Boer	human ignition	pre-industrial	–	pre-industrial	1948–1972
C-AB-HI-FS	Arora and Boer	human ign. and fire suppr.	pre-industrial	–	pre-industrial	1948–1972
Transient simulations: 1798–2004						
T-FULL	Thonicke	–	–	transient	transient	1948–1972/1973–2004
AB-FULL	Arora and Boer	constant=0.5	–	transient	transient	1948–1972/1973–2004
AB-HI	Arora and Boer	human ignition	transient	transient	transient	1948–1972/1973–2004
AB-HI-FS	Arora and Boer	human ign. and fire suppr.	transient	transient	transient	1948–1972/1973–2004
Sensitivity simulations: 1798–2004						
AB-LUC	Arora and Boer	constant=0.5	–	–	transient	1948–1972/1973–2004
AB-CLIM	Arora and Boer	constant=0.5	–	transient	transient	1948–1972
AB-HI-PI	Arora and Boer	human ignition	pre-industrial	transient	transient	1948–1972/1973–2004
AB-HI-FS-PI	Arora and Boer	human ign. and fire suppr.	pre-industrial	transient	transient	1948–1972/1973–2004

¹ Fire algorithm: in CLM-CN based on Thonicke et al. (2001) or Arora and Boer (2005).

² different treatment of human ignition: either a constant value of 0.5 (constant), or following a human ignition only (HI) or human ignition and fire suppression scenario (HI-FS).

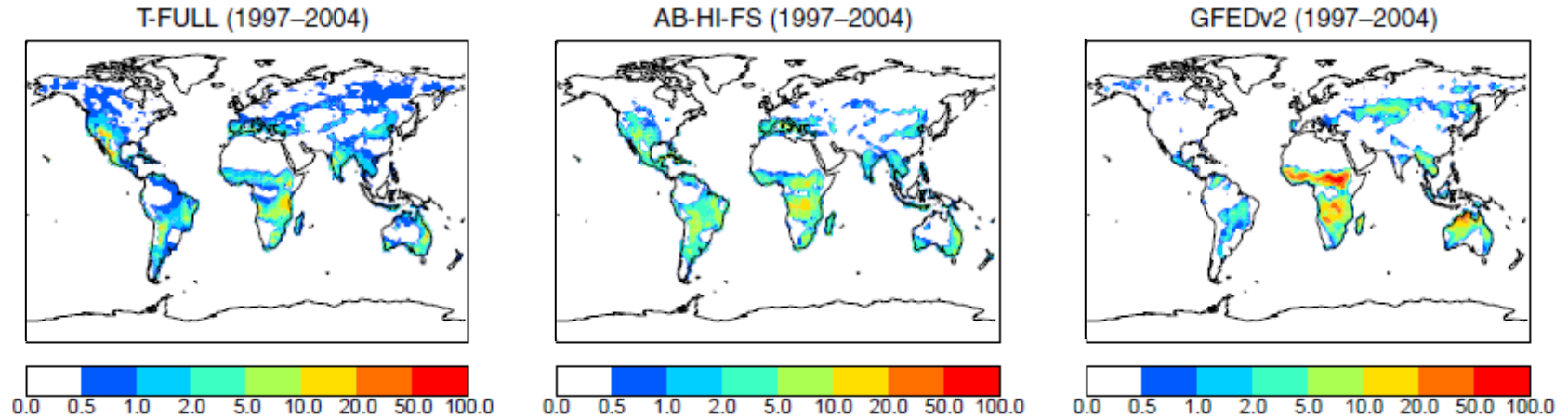
³ Population density is considered transient between 1798 and 2004 (Klein Goldewijk, 2001) or held constant at a pre-industrial value (PI),

⁴ Land cover change and wood harvest: either no land cover change and wood harvest (–) or transient land cover change and wood harvest between 1850–2004 (Hurtt et al., 2006).

⁵ CO₂ concentration and nitrogen deposition are set to pre-industrial values for the control simulations and are transient time-varying for the transient simulations.

⁶ Climate forcing: either cycling periodically through NCEP/NCAR data (Qian et al., 2006) for the years 1948–1972 or cycling through 1948–1972 followed by the full time series for the years 1948–2004.

Contemporary global patterns of burned area have improved



% of grid cell burning during 1997-2004

Table 2. Annual mean total (wildfire and deforestation) fire carbon emissions and annual burned areas for Africa (NHAF: Northern Hemisphere Africa, SHAF: Southern Hemisphere Africa) for the different simulations compared to observations. All reported values are averages over the years 2001–2004.

	L3JRC	GFEDv2	Lehsten et al. (2009)*	T-FULL	AB-FULL	AB-HI	AB-HI-FS
area burned [Mha]							
SHAF	87.4±8.0	80.0±3.5	112±15.3	39.0±2.6	74.1±8.0	66.0±7.3	45.45±2.5
NHAF	68.0±7.8	139±10.3	86.7±9.6	19.5±0.5	44.5±2.7	43.8±3.5	26.4±5.2
carbon loss [Tg C/yr]							
SHAF		577±14.0	457±81.8	402±21.5	504±38.1	537±37.6	414±39.8
NHAF		621±69.0	280±36.7	308±21.2	490±79.5	510±88.9	367±71.3

* Lehsten et al. (2009) uses burned areas as reported in L3JRC modified by a correction term to compensate for a likely underestimation.

Global burned area increases with Aurora and Boer algorithm

Table 3. Annual mean carbon in the above ground vegetation pools (deadstem, livestem, leaves, coarse woody debris and litter), annual burned area, and ratio between annual carbon loss and burned area in steady state for the different simulations.

	above veg.	annual burned area	annual carbon emission/ burned area
simulation	[Pg C]	[Mha]	[Tg C/Mha]
T-FULL	722	136	16.3
AB-FULL	579	300	8.5
AB-HI	649	194	9.4
AB-HI-FS	659	182	9.8

- Global burned area from GFEDv3 is 370 Mha (Giglio et al. (2010) Biogeosciences Discussions
- Giglio reference: <http://www.biogeosciences-discuss.net/6/11577/2009/bgd-6-11577-2009.pdf>

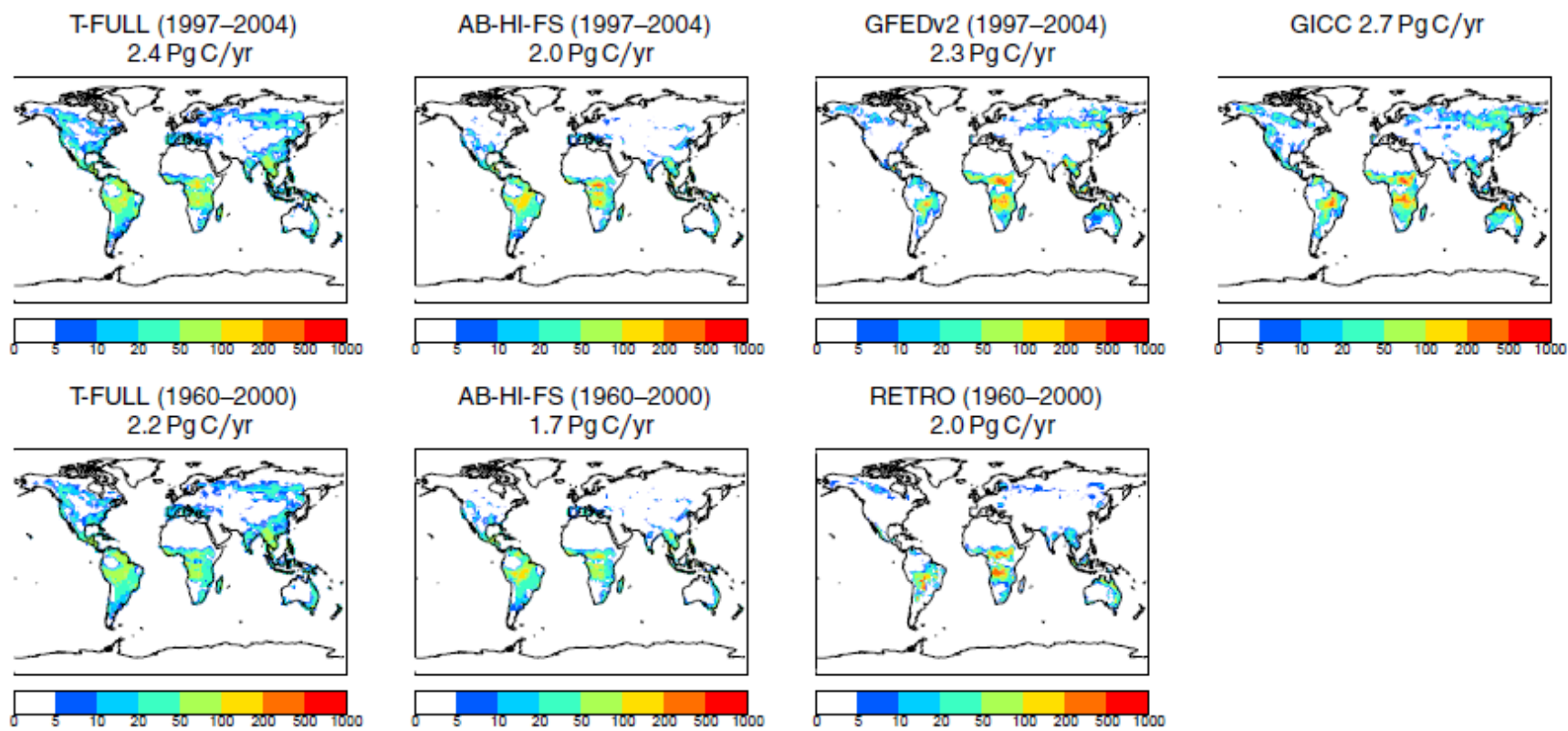


Fig. 3. Annual mean total (wildfire plus deforestation) fire carbon emissions [$\text{g C/m}^2/\text{year}$] compared to emissions reported in the fire products GFEDv2 (van der Werf et al., 2006), RETRO (Schultz et al., 2008) and GICC (Mieville et al., 2010). The model simulations are averaged over the corresponding observational periods (GFEDv2/GICC: 1997–2004; RETRO: 1960–2000). Numbers report global total carbon emissions. Regional values for all simulations performed are given in Fig. 4.

Model simulates reasonable interannual variability of global fire emissions

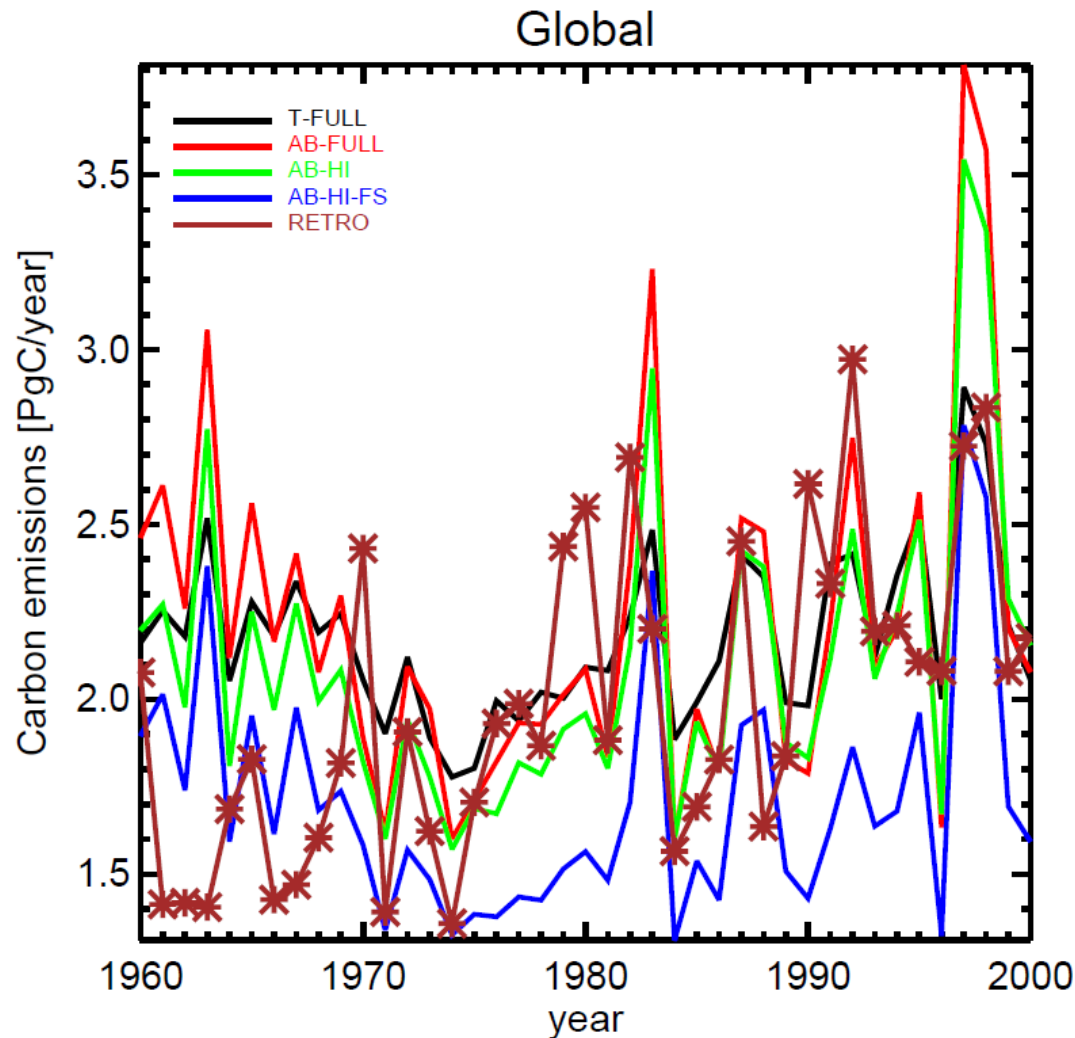
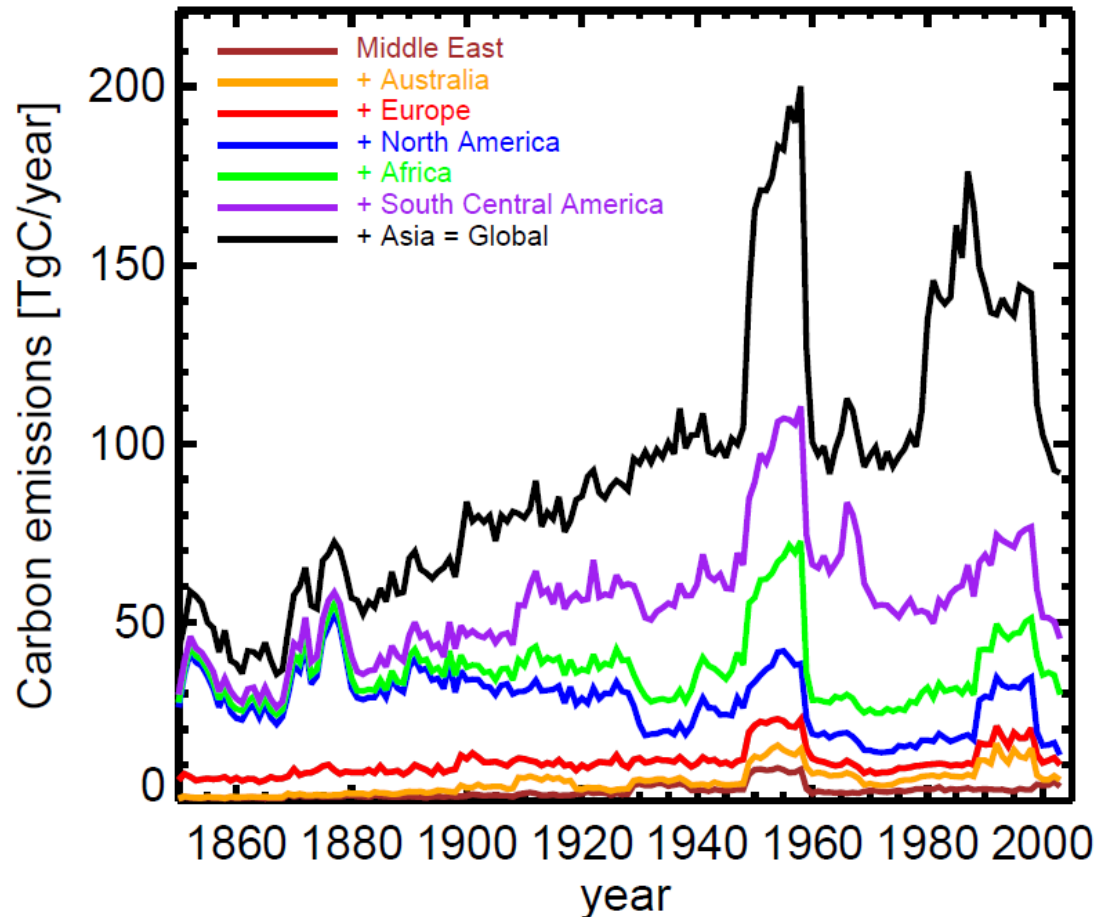


Fig. 11. Annual mean total (wildfire and deforestation) fire carbon emissions in [PgC/year] for the different simulations from 1960–2000 compared to values reported in RETRO (Schultz et al., 2008).

Deforestation fire emissions now vary seasonally and interannually with climate



Currently 11% of deforestation carbon losses occur as fire emissions
Likely number closer to 50% -> GFEDv2 deforestation fires are $\sim 0.3 - 1.0$ Pg C/yr

Conclusions

- The last three decades in the 20th century are dominated by an upward trend in global total fire carbon emissions (+30%) caused by climate variations and large burning events associated with ENSO induced drought conditions.
- Land use change activities between 1850 and 2000 lead to simulated total carbon emissions from deforestation fires of 14 Pg C, but reduced carbon emissions from wildfires by 24Pg C. Thus, total (wildfire and deforestation) fire carbon emissions are reduced by 10 Pg C (-3%).
- The net flux of carbon to the atmosphere due to land use activities is simulated as 1.2 Pg C/year for 1990–1999 (similar to previous estimates in *Ito et al.*, 2008; *Shevliakova et al.*, 2009). For 2000–2004 this source decreases from 1.20 to 0.85 PgC/year. 11% of this source is in the model attributed to deforestation fires.

Next steps

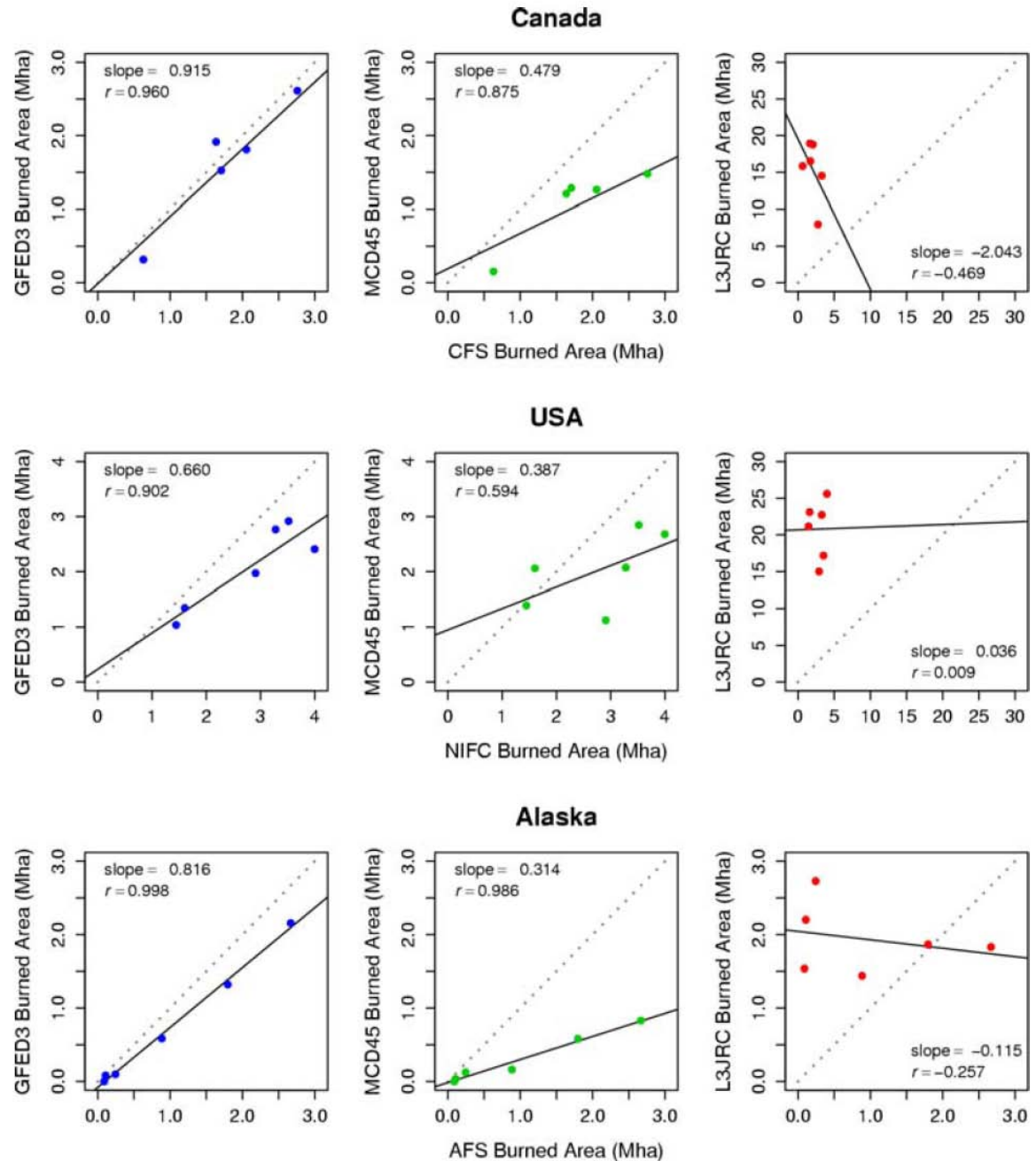
- Migrate Kloster's improved fire algorithm to CLM-CN version 4
 - Reassess in context of proposed adjustments to wood harvesting
 - Need to improve climate driving datasets for transient simulations for 20th century
- Allow fires to change the distribution of PFTs within a grid cell
- Examine fire-climate feedbacks!
 - CO₂ emissions
 - Aerosols
 - Ozone
- Examine fire contributions to global redistributions of N and P

Table A3. The redistribution of carbon and nitrogen upon conversion used in CLM-CN. Factors are based on Houghton et al. (1983).

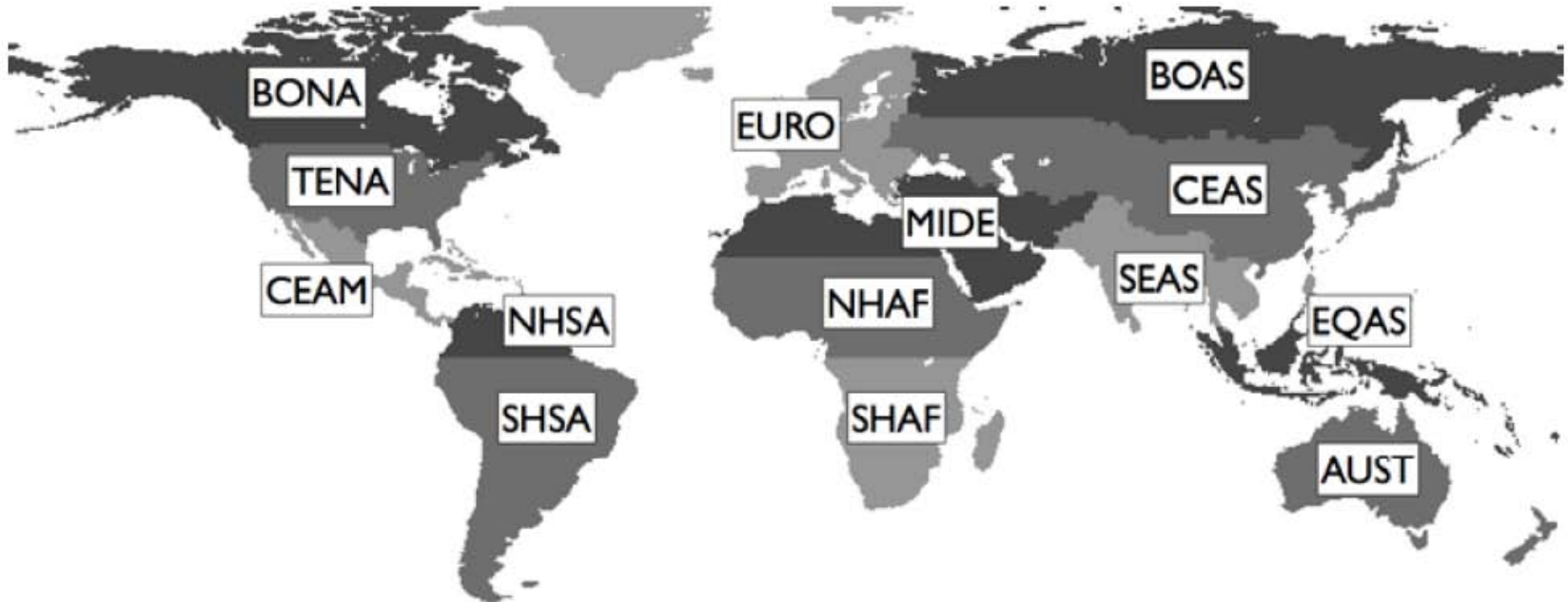
Ecosystem	conversion flux	paper product pool	wood product pool
Temperate/boreal forest	0.60	0.30	0.10
Tropical forest	0.60	0.40	0.00
Grassland	1.00	0.00	0.00
Shrub lands	0.80	0.20	0.00

Global burned area

- Where available, we use 500-m burned area maps produced by a change detection algorithm with surface reflectance from MODIS
- Burned area extended to other periods and area by relating this burned area product in each region to active fire detections from MODIS, VIRS, and ATSR instruments



Regions of analysis



BONA Boreal North America
TENA Temperate North America
CEAM Central America
NHSA Northern Hemisphere South America
SHSA Southern Hemisphere South America
EURO Europe
MIDE Middle East

NHAF Northern Hemisphere Africa
SHAF Southern Hemisphere Africa
BOAS Boreal Asia
CEAS Central Asia
SEAS Southeast Asia
EQAS Equatorial Asia
AUST Australia and New Zealand

